XLVI CILAMCE
VITÓRIA - ES - BRAZIL - 2025
XLVI IBERO-LATIN AMERICAN CONGRESS ON COMPUTATIONAL METHODS IN ENGENEERING

Vibration analysis of an extremely flexible beam with concentrated load axially stressed by incremental force

Iago G. de Oliveira[1], Alexandre de M. Wahrhaftig[2], Mariely de J. Neri[3], Eduardo M. de O. Lopes[4], Kevin M. M. Ribeiro[5], José M.Balthazar[6]

[1,2]*Graduate Program in Civil and Environmental Engineering, University of Feira de Santana* (*UEFS*)
Av. Transnordestina, SN–Novo Horizonte, Zip-Code: 44036-900, Feira de Santana, Bahia, Brazil
iago23299@gmail.com
[2]*Dept. of Constructions and Structures, Polytechnic School, Federal University of Bahia* (*UFBA*)
Rua Aristides Novis, 02 – Federação, Zip-Code: 40.210-910, Salvador, Bahia, Brasil
alixa@ufba.br
[3]*Institutional Scientific Initiation Program* (*PIBIC/UFBA*), *Dept. of Constructions and Structures, Polytechnic School, Federal University of Bahia* (*UFBA*)
Rua Aristides Novis, 02 – Federação, Zip-Code: 40.210-910, Salvador, Bahia, Brazil
mariely.neri@ufba.br
[4,5]*Dept. of Mechanical Engineering, Technology Sector, Federal University of Paraná* (*UFPR*)
Av. Cel. Francisco H. dos Santos, 100 – Jardim das Américas, Zip-Code: 81530-000, Curitiba, Paraná, Brazil
[4]*eduardo_lopes@ufpr.br*, [5]*eng.kevin.mmr@gmail.com*
[6]*Dept. of Mechanical Engineering, Faculty of Engineering, São Paulo State University* (*UNESP*)
Av. Eng Luiz Edmundo Carrijo Coube, 14-01, Zip-Code: 17033-360, Bauru, São Paulo, Brazil
manoel.balthazar@unesp.br

Abstract. Cables have been fundamental instruments in human development. They were used in prehistoric times as tools in activities essential to human survival and are currently employed in modern structures, such as supporting cable-stayed bridges and prestressed beams. In today's world, overhead cables are essential for the transmission of electricity and the internet. From a structural standpoint, overhead cables can be associated with highly flexible beams subjected to a tensile force. The tensile force alters the cable's dynamics, whose natural vibration frequencies depend on the intensity of the applied force. In practical situations, the tensile force is transferred to the cable incrementally, dividing the final value into installments that accumulate in the structure until the final value is reached. Successive increments gradually reduce the deformation the cable assumes under the influence of gravity. Therefore, as the tensile force increases, a new equilibrium condition is established, and new equations become necessary. For transmission lines, exposure to wind can favor resonance. In this case, the use of vibration attenuators composed of localized masses has been the most widely adopted strategy. To study the vibration of a cable modeled as a beam, subjected to concentrated vertical forces and incrementally tensioned, a mathematical solution based on the Rayleigh method was developed. The equations were implemented in Python. The routine defines the shape of the cable at each increment of the tension force and then uses it as the shape function of the dynamic method. Finally, comparisons are made with the system when free of concentrated vertical forces.

Keywords: incremental force, vertical force, overhead cables, numerical solution, natural frequency of vibration.

1 Introduction

Overhead cables play a crucial role in modern engineering, being essential in applications such as power transmission lines, cable-stayed bridges, and prestressed beams. Their importance lies in their ability to support loads with structural efficiency, ensuring safety and performance in various infrastructure systems. Cables are

slender and flexible structural elements, whose equilibrium is only possible in the deformed configuration of the system. In general, for proper operation, overhead cables must be tensioned during line installation. The application of a tensile force modifies the natural frequencies of the cables, as it adds the geometric stiffness (Wahrhaftig [1]) to the total stiffness of the system (Wahrhaftig [2]). Souza et al. [3] emphasize that geometric stiffness plays a crucial role in determining the natural frequency of cable structures, as they only offer resistance when subjected to axial tensile forces, which are directly reflected in the shape and vibration frequencies.

Hijmissen et al. [4] studied the effect of bending stiffness on the damping properties of tensioned cables. They demonstrated that the inclusion of tuned mass dampers (TMDs) can attenuate vibrations induced by external excitation. However, they observed that cable bending alters the natural frequencies of the cable, reducing the effectiveness of the TMD. To overcome this limitation, they recommended adjustments to the attenuator's spring constant, ensuring better performance in controlling oscillations. Zhu [5] investigated the damping in slack cables without axial loading, using a model based on homogenized Rayleigh damping. The author concluded that bending caused by friction between the cable strands greatly influences the dynamic behavior of these structures. Impollonia et al. [6] developed a closed-form solution in vector representation for the catenary problem in elastic cables, encompassing both distributed loads and point forces oriented in space. The solution allowed for the precise determination of the cable's deformed configuration, representing an evolution of classical approaches and offering greater computational efficiency in three-dimensional modeling. Ribeiro et al. [7] developed a closed-form analytical solution for the frequency response function with parametric identification of the stiffness and internal damping of overhead cables.

Chang et al. [8] performed an analysis of the nonlinear dynamic behavior of an elastic cable, using catenary theory to model cable deformation under different loading conditions. The authors used the finite element method to simulate the cable's behavior in different dynamic scenarios, considering the complexity of the interactions between internal forces, material elasticity, and system geometry. Manuel et al. [9] used Python as a tool for numerical simulation based on the finite element method, developing a code that receives input data and solves the relevant problems, discretizing the results into a two-dimensional mesh. Zaman [10] also used Python to numerically solve elliptic partial differential equations, widely applied in complex structural problems. Oliveira et al. [11] analyzed the vibrational behavior of an extremely flexible cable, tensioned by an incremental force and considering the viscoelastic effect of the material, but disregarding the presence of concentrated vertical loads.

In this work, the influence of concentrated vertical loads arranged along a cable modeled as a beam and subjected to incremental axial tensile force is studied. The vibration frequencies at each force increment are determined. Comparisons with a system free of vertical forces are also presented.

2 Description of the problem and study

2.1 Context

Consider the cable represented, generically, in Fig. 1(a), subjected to distributed loads, q, and concentrated loads, c, and having as essential properties its flexural stiffness, EI, and mass per unit length, $\overline{m}$. Under the influence of these loads, the structure deforms, presenting a configuration known as *Elastica* [12]. The complete solution is attributed to Euler because of his compelling mathematical treatment [13]. The approximate equation of the elastic line represents the starting point for estimating the vibration frequency of this system. The displacements relative to the straight axis, which define the elastic line of the beam, are given by a polynomial function in x, designated by $y(x)$, whose origin is located at support B, and is valid in the beam domain, i.e., $0 \leq x \leq L$, Fig. 1(b). Fig. 2 illustrates two identical models, except for the concentrated forces, c, applied to the second model. The deformation, in both cases, is obtained by determining the equilibrium of the internal and external forces in the intervals defined by the load distribution. In the first case, only one section needs to be adopted, while in the second, four intervals are necessary to complete the formulation of the problem, which are reduced to two if one takes advantage of the symmetry of the system. In the first model, Fig. 2(a), the deformation is calculated considering only a single section ($0 \leq x \leq L$), since there is no variation in load along the structure. In the second model, shown in Fig. 2(b), the deformation is determined in two sections ($0 \leq x < L/4$, and $L/4 \leq x \leq L/2$), due to the symmetry of the problem. Once the equilibrium of forces is established, the integration of the bending moment equation in each interval with respect to x results in expressions for the angle of rotation of the beam in these same intervals.

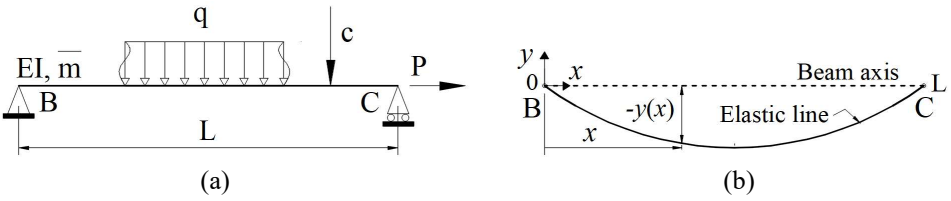


Figure 1. Generic modeling of the problem (a) and representation of the elastic line (b)

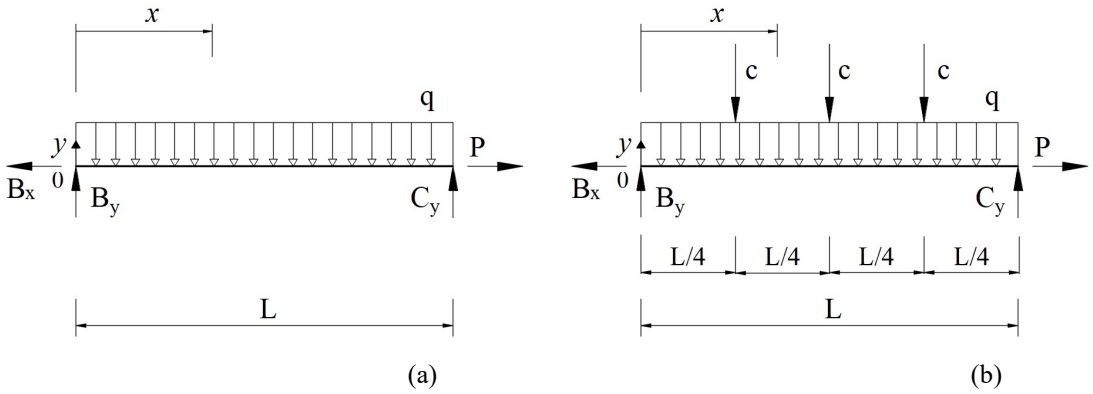


Figure 2. (a) model 1: only distributed loading; (b) model 2: with concentrated and distributed loading

The equations so obtained describe the variation of internal force and the slope of the tangent straight to the elastic line along the length of the structural element, at different positions x, and are valid in the intervals reserved for them. The integration of the rotation equations leads to expressions that represent the deformation of the beam, providing a detailed description of the vertical displacement of the points along its axis. The integration constants that arise at this process are determined by the boundary conditions particular to each problem. One of them is the zero displacement upon support B, where x is equal to zero. Another is the rotation angle, also zero, at midspan, where $x = L/2$. The other constants are determined by equating the expressions for rotation and displacement at the boundary position where $x = L/4$, established for the intervals immediately before and after this position. By imposing the restrictions of the existing intervals, a single equation for the bending moment, $M(x)$, for the rotation, $\theta(x)$, and for the displacements, $y(x)$, is obtained, which can be used to represent these parameters throughout the beam domain. In that representation, the utilized convention considers the positive bending moment forcing the concavity of the beam to face upwards, i.e., producing negative displacements of the beam axis.

2.2 Natural frequency of vibration

In determining the natural frequency, the Rayleigh method [14] is used. In this procedure, the function $y(x)$ to be used is the one compatible with each model studied. The stiffness components of model 1 are the flexural stiffness, k_0, eq.(3), and the geometric stiffness, k_G, eq. (4).

$$k_0 = \int_0^L EI\left(y''(x)\right)^2 dx \tag{3}$$

$$k_G = P\int_0^L \left(y'(x)\right)^2 dx \tag{4}$$

In model 2, these stiffnesses are calculated for the segments to the left of the symmetry line, that is, from the center of the beam ($0 \le x < L/4$ and $L/4 \le x \le L/2$). Eqs. (5) and (6) represent the parcels of the bending stiffness (k_0) and the geometric stiffness (k_G) for this model.

$$k_0 = 2\int_0^{L/4} EI\left(y''(x)\right)^2 dx + 2\int_{L/4}^{L/2} EI\left(y''(x)\right)^2 dx \tag{5}$$

$$k_G = 2P\int_0^{L/4}\left(y'(x)\right)^2 dx + 2P\int_{L/4}^{L/2}\left(y'(x)\right)^2 dx \tag{6}$$

The total stiffness of both models, K, upper letter, is given by eq. (7).

$$K = k_0 + k_G \tag{7}$$

The contribution of the distributed mass, m_d, is calculated by eq. (8):

$$m_d = \int_0^L \bar{m}\left(y(x)\right)^2 dx \tag{8}$$

where $\bar{m} = q/\mathrm{g}$ is the mass per unit length, g is the acceleration of gravity. The concentrated masses are calculated by eq. (9):

$$m_C = \sum_n m_c\left(y(x_{cn})\right)^2 \quad \text{with} \quad m_c = c/g \tag{9}$$

where x_{cn} indicates the position occupied by the concentrated vertical force c_n (n = 1, 2). The expression for the total generalized mass, eq. (10), corresponds to the sum of equations (8) and (9), according to the procedure presented by Wahrhaftig and Brasil [15]. Therefore,

$$\Pi = \int_0^L \bar{m}\left(y(x)\right)^2 dx + \sum_n m_c\left(y(x_{cn})\right)^2 \tag{10}$$

The frequency can then be obtained by the square root of the ratio of total stiffness, K, eq. (7), which consider both parcels, the flexural and geometric, to the generalized mass, eq. (11), whether for model 1 or 2. In the first case, $c = 0$.

$$\omega = \sqrt{\frac{K}{\Pi}} \text{ (in rad/s)} \quad \text{and} \quad f = \frac{\omega}{2\pi} \text{ (in Hertz)} \tag{11}$$

It is of interest to mention that in comparison with computational modelling through the finite element method (FEM), negligible differences of 0.0003% and 0.0069% were found for displacement and frequency, respectively, [16] in relation to results produced by the current mathematical procedure. This quality of results is possible because the condition imposed to the analytical method is the obedience of the shape function to the essential boundary conditions of the problem [17]. Even being an acceptable tool, results computed by finite element method contain error, which can be understood as a difference between the computational results and the exact solution given by the mathematical model [18]. Therefore, the solution of reference is the analytical one, not the contrary.

2.3 Iterative process

The shape equation for each section is initially formulated for vertical forces only. By introducing an axial force in the deformed state, the equilibrium bending moments are calculated, requiring the sum to be zero. The iterative solution of the elastic line must consider the deformations at each increment i of the tensile force. The change in the cable shape follows an iterative numerical model, in which the current moment is adjusted by subtracting the bending moment generated by the increment in the axial force, as per eq. (12), applied to as many sections as necessary.

$$M_i = M(x)_0 + \Delta P\sum_{i=1}^{n} z(x)_{i-1} \tag{12}$$

To solve the problem, a computational routine was developed using the *Python* language, employing three main libraries: *sympy*, *numpy*, and *matplotlib.pyplot*. The *sympy* library was responsible for symbolic manipulation, allowing the definition of equations and variables, and the performance of operations such as integrals and algebraic resolutions. *Numpy* was used for numerical operations, especially in generating x-values with the *np.linspace* function, a data preparation step. Finally, *matplotlib.pyplot* was used for graphical visualization of the results, allowing the plotting of the calculated functions.

On this *script*, 21 iterations were performed on a notebook with the following characteristics: CPU Intel core i5-8265U de 3.2 GHz; 16 GB de ram; 2 TB de HD; 1 TB de SSD; GPU 0 Intel(R) UHD Graphics 620; GPU 1 Radeon 520 de 2GB. The processing time for the total number of iterations, with the described configuration, was 0.15 hours for model 1 and 2.15 hours for model 2. The computational process occurs as a function of the while loop, for which the condition while $\Sigma \Delta P \leq P$ keeps the computational processing in an active cycle, as described in the flowchart in Fig. (3).

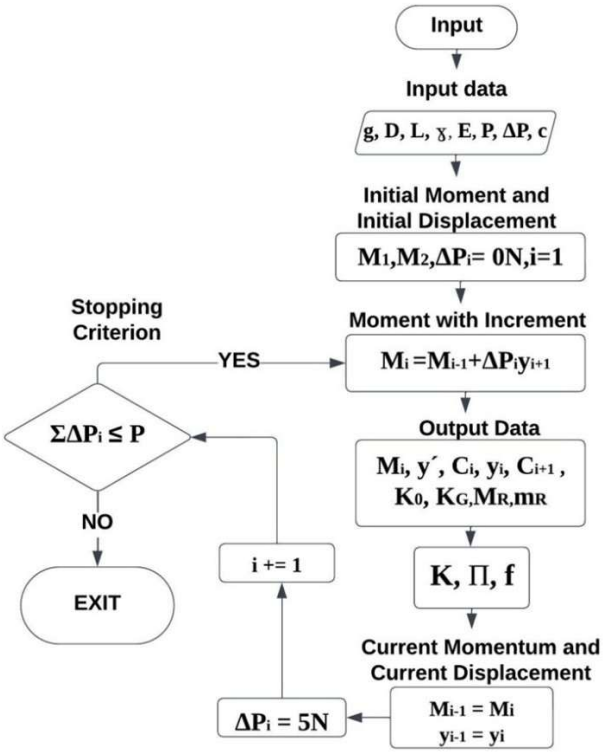


Figure 3. Programming flowchart

3 Numerical simulation, results and discussion

The data used in the numerical simulation are shown in Tab. 1. The bending moments are presented in Fig. 4(a) for model 1 and in Fig. 5(a) for model 2. A progressive reduction of these functions can be observed with each increase in the tensile force. It can be seen that the cable tends to align itself horizontally, reducing the rotations in the cross sections, as illustrated in Fig. 4(b) and Fig. 5(b). A decrease in displacements is also observed, Fig. 4(c) and Fig. 5(c), with each step of increase in the horizontal force. In turn, the natural frequency of vibration, obtained under the effect of the loadings, increases proportionally to the applied tensile force, as illustrated in Figs. 6(a) and 6(b). This is due to the increase in the stiffness of the system conferred by the geometric portion. Since the Rayleigh method uses the elastic line of the beam as a shape function, each iteration represents a new equilibrium configuration, simultaneously modifying the stiffness and the generalized mass of the system.

Table 1. Input data

Parameter	Value
Acceleration of gravity, g, (m/s^2)	9.807
Cable diameter, d, (m)	0.0183
Cable length, L, (m)	13.385
Mass per unit length, $\bar{m}$, (kg/m)	0.813
Apparent modulus of elasticity of the cable, E, (N/m^2)	65×10^9
Ultimate tensile force, P, (N)	100
Increase in traction force, ΔP, (N)	5
Concentrated vertical force, c, (N)	25

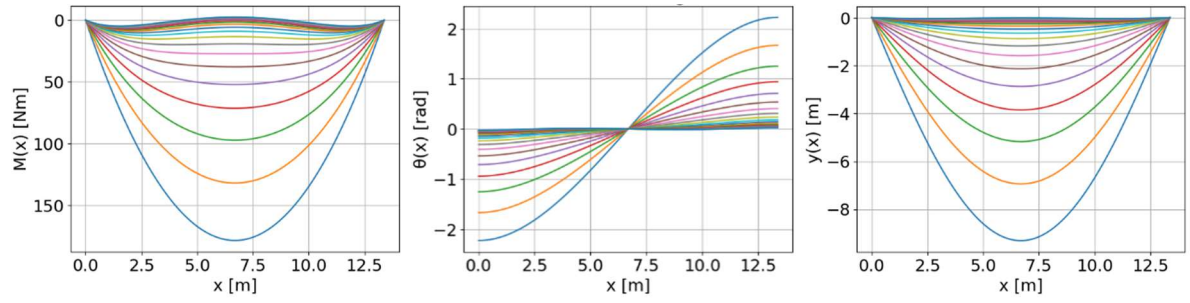


Figure 4. Diagrams of model 1: (a) Bending moment, (b) Rotation of cross sections, (c) Vertical displacement

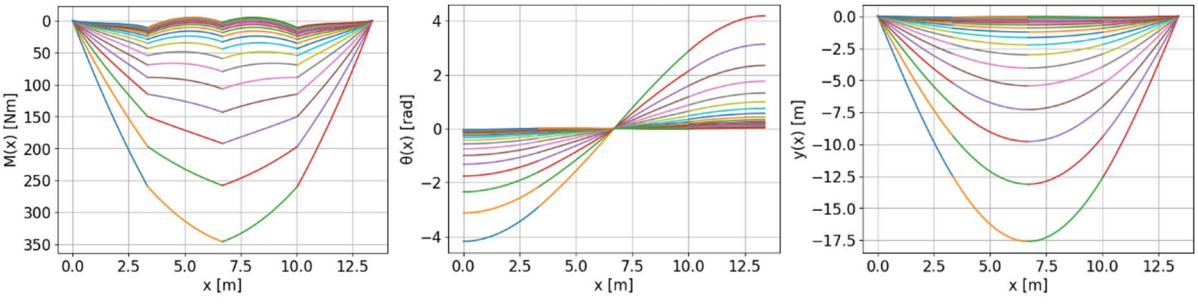


Figure 5. Diagrams of model 2: (a) Bending moment, (b) Rotation of cross sections, (c) Vertical displacement

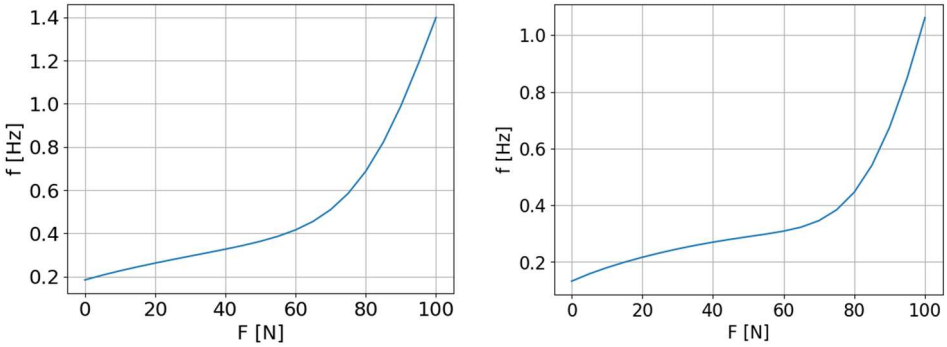


Figure 6. Natural frequency of vibration: (a) model 1, and (b) model 2.

4 Conclusions

This study analyzed the variation in the natural vibration frequency of a cable modeled as a beam and subjected to incremental tensile force. A comparative analysis was performed between two models. The first was free of concentrated vertical forces, while the second had three such forces. Both models were subjected to their own weight. The following conclusions can be drawn:

- From a computational perspective, there was a significant difference in analysis time between the two models. The first required 0.15 hours to complete, while the second required 2.15 hours. It is assumed that the number of intervals in determining equilibrium at the various sections, and therefore in defining the beam's deformation, results in a greater number of equations to be calculated at each iteration step.
- The comparison of results from the two models made it possible to verify that the bending moment, the rotation angle and the deformation increase with the increase in concentrated vertical loads.

- At the initial iteration, the model without concentrated loads presented a vertical displacement of 9.31 m, while to the model with concentrated loads it was 12.09 m, an increase of approximately 30% (29.86%).
- The final value of the natural vibration frequency decreases with the insertion of concentrated vertical forces into the system. model 1 presented a vibration frequency at the end of the iterative process of 1,3994 Hz, and model 2 of 1.0618 Hz, a reduction of more than 24% (24.13%). This decrease was due to the increase in mass, resulting from the insertion of the three concentrated loads.
- The natural vibration frequencies of both model 1 (without concentrated forces) and model 2 (with concentrated forces) increase nonlinearly with the axial tensile force at each iteration step. Therefore, this is a problem with a nonlinear response, originally based on the assumption of geometric linearity.

Acknowledgements. The authors would like to thank UEFS (State University of Feira de Santana), UFBA (Federal University of Bahia), FAPESB (Bahia State Research Support Foundation), and CNPq (National Council for Scientific and Technological Development) for all support given.

Authorship statement. The authors hereby confirm that they are the sole liable persons responsible for the authorship of this work, and that all material that has been herein included as part of the present paper is either the property (and authorship) of the authors, or has the permission of the owners to be included here.

References

[1] Wahrhaftig, A., Dantas, J., Brasil, R. and Kloda, L., 2022a, "Control of the Vibration of Simply Supported Beams Using Springs with Proportional Stiffness to the Axially Applied Force". *J Vib Eng Technol*, 10, 2163–2177.
[2] Wahrhaftig, A., Magalhães, K., Silva, M., Brasil and R, Banerjee, J., 2022b, "Buckling and free vibration analysis of non-prismatic columns using optimized shape functions and Rayleigh method". *Eur J Mech - A/Solids*, 94, 104543.
[3] Sousa, R., de Souza, R., Neto, J. and Júnior, G., 2005. Análise de Vibrações em Cabos Considerando a Rigidez à Flexão, a Rigidez ao Cisalhamento e a Inércia à Rotação da Seção. In: CILAMCE2005, Guarapari, Brazil.
[4] Hijmissen, J. W., Heuvel, N. W. and Horsen, W. T., 2009. "On the effect of the bending stiffness on the damping properties of a tensioned cable with an attached tuned-mass-damper". *Eng.Struc.*, Vol. 31, pp. 1276-1285.
[5] Zhu, Z. H. and Meguid, S. A., 2007. "Nonlinear FE-based investigation of flexural damping of slacking wire cables". *Int. J. Solids Struct.*, Vol. 44, pp. 5122-5132.
[6] Impollonia, N., Ricciardi, G., and Saitta, F., 2011. "Statics of elastic cables under 3D point forces". *Int. J. Solids Struct.*, Vol. 48, pp. 1268-1276.
[7] Ribeiro, K. M. M., Amaral, G. R. D., Balthazar, J. M., Wahrhaftig, A. M. and Lopes, E. M. D. O., 2025. "On the experimental and numerical determination of dynamic parameters of overhead power cables. *Acta Mech.*, Vol. July 1-29.
[8] Chang, B. S., Park, J. and Lee, K., 2008. "Nonlinear dynamic analysis of spatially suspended elastic catenary cable with finite element method". *KSCE J. Civ. Eng*, Vol. 12, pp. 121-128.
[9] Manuel, P. A., Arjona, M. A., Hernandez, C. and Escarela-Perez, R., 2023. "Numerical Modeling and Analysis of an Electromagnetic Device Using a Weakly Coupled Magnetostatic-Mechanical Formulation and the 2D Finite Element Method". *Energies*, Vol. 16.
[10] Zaman, M. A., 2022. "Numerical Solution of the Poisson Equation Using Finite Difference Matrix Operators". *Electronics Switzerland*, Vol. 11.
[11] Oliveira, I. G., Wahrhaftig, A. M., Menezes, C. M. and Lopes, E. M. O., 2024. "Vibration of extremely flexible beam axially tensioned by incremental force". In: Proceedings of the XLV Ibero-Latin-American Congress on Computational Methods in Engineering – CILAMCE 2024, Maceió, Brazil.
[12] Levien, R., 2008, "The elastica: a mathematical history", University of California, Berkeley, USA.
[13] Euler, L., 1744. "De Curvis Elasticis, "Additamentum I to his Methodus Inveniendi Lineas Curvas Maximi Minimive Proprietate Gaudentes". Lausanne and Geneva.
[14] Strutt , J.W. (3rd Baron Rayleigh - 1877). *Theory of Sound*. Dover Publications, pp. 522, New York, re-issued, 1945.
[15] Wahrhaftig, A. M, and Brasil, R. M. L. R. F., 2017, "Vibration analysis of mobile phone mast system by Rayleigh method". *Appl. Math. Model.*, Vol. 42, pp. 330–345.
[16] Wahrhaftig, A. M., Oliveira, I. G., Conceição, R. O. S., Menezes, C. M., Lopes, E. M. O., Ribeiro, K. M. M., Amaral, G. R. and Balthazar, J. M., 2023. "Study of the first mode of vibration of transmission line cables via Rayleigh's method and elastic line equation". In: 27th Intern. Congress of Mechanical Engineering – CONEM 2023, Florianopolis, SC, Brazil.
[17] Ilanko, S., Monterrubio, L. E. and Mochida, Y., 2014. "The Rayleigh−Ritz Method for Structural Analysis". John Wiley and Sons, Inc, Madison, USA.
[18] Cook, R. D., Malkus, D. S., Pleshe, M. E. and Witt, R. J., 2002. "Concepts and Applications of Finite Element Analysis". 4th Ed., NJ: John Wiley and Sons, Inc, Madison, USA.